The conformational analysis of phosphine ligands in organometallic complexes. Part 1. Triphenylphosphine coordinated to an achiral metal centre[1]

James F. Costello *,[a] **and Stephen G. Davies** *,[b]

[a] *Department of Chemistry, University of the West of England, Coldharbour Lane, Bristol, UK BS16 1QY*
[b] *Dyson Perrins Laboratory, University of Oxford, South Parks Road, Oxford, UK OX1 3QY*

The conformational analyses of PPh_3 1 and the representative achiral metal complexes $[Al(PPh_3)(Me)_3]$ 2, $[Fe(PPh_3)(CO)_4]$ 7 and $[Ir(PPh_3)_2(CO)_3]^+$ 8 possessing tetrahedral and trigonal-bipyramidal geometries are reported, and comparisons between the calculated and solid-state structures are made. The intramolecular non-bonded interactions which govern the conformational preferences of PPh_3 in both the free and complex-bound state are characterised. The equilibrium between the opposing inter ring–ring and inter ring–ligand interactions which govern the minimum energy conformations of these complexes is examined. Analysis of the conformational preferences of PPh_3 ligands in metal complexes is facilitated by the introduction of the novel concept of the plane of nadir energy.

As ligands, phosphines provide a versatile tool for the control of both the structure and reactivity of transition metal complexes. Triphenylphosphine **1** is a ligand ubiquitous in organometallic chemistry and a generalised model for the conformational preferences of this molecule when attached to metal centres should provide a contribution to the development of improved reagents and catalysts. Triphenylphosphine **1** may adopt two high energy achiral conformations, both of which possess C_{3v} symmetry. Firstly, the plane defined by the atoms of each phenyl ring may lie perpendicular to the plane described by the three C_i (C_{ipso}) atoms (hereon referred to as the reference plane). Secondly, the plane of each phenyl ring may lie *flat*, thereby orienting all six C_o (C_{ortho}) atoms equidistant from, and on the same side of, the reference plane. Both of these arrangements incur unfavourable $H_o \cdots H_o$ interactions; the latter case is particularly destabilised because all six H_o atoms invoke a steric penalty.[2] Therefore, in order to minimise these intramolecular interactions, a correlated feathering of the phenyl propellers occurs in both the free and the complex-bound state. Each phenyl group twists about the P–C_i bond in the same sense so that the basic framework now possesses C_3 symmetry. The vector perpendicular to the reference plane and incident upon the P atom is thus recognised as an axis of chirality. The helicity, or propeller chirality, in **1** can therefore be described[3] in terms of two enantiomeric configurations, *i.e. clockwise* (*P*) and *anti-clockwise* (*M*), respectively (Fig. 1). The two enantiomeric configurations of **1** may undergo stereoisomerisation by a two-ring flip mechanism, facilitated by correlated rotations about the P–C_i bonds.[4]

When **1** is attached to an achiral metal centre, the two complexes formed are enantiomers and hence being degenerate occur in equal amounts. The enantiomeric complexes interconvert *via* rapid low energy intramolecular processes.[5] Although structural correlations[6,7] and molecular mechanics calculations[8] have been reported, limited success has been achieved in developing a general model[1] which includes an account of the intramolecular interactions associated with the propeller conformations of PPh_3 ligands attached to achiral metal centres. In organometallic complexes containing **1**, the conformation of the three phenyl rings in the crystal is primarily determined by intramolecular steric interactions.[9] Molecular modelling studies using the Chem-X† package, which employ van der Waals interaction energy calculations, have proven remarkably successful in determining the accessible conformations of a variety of organometallic complexes.[10] As a prelude to the study of more complicated systems,[1] we present a conformational analysis of **1**, in both the free, and

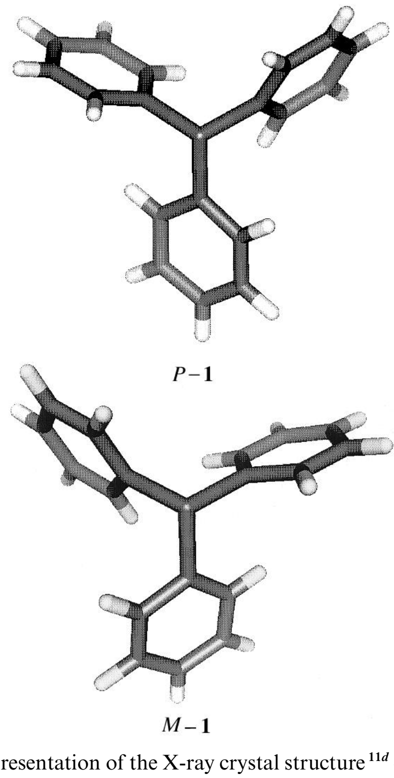
P−**1**

M−**1**

Fig. 1 A representation of the X-ray crystal structure[11d] of **1** as viewed along the σ_{nb}–P axis, demonstrating the enantiomeric configurations *P* and *M*, respectively

---

† Chem-X, designed and distributed by Chemical Design Limited, Roundway House, Cromwell Park, Chipping Norton, Oxfordshire, UK OX7 5SR.

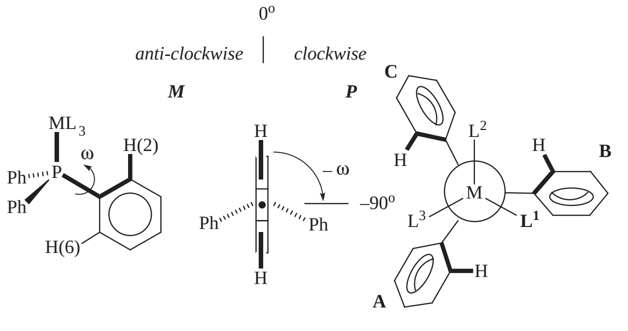

(a) (b) (c)

Fig. 2 Definition of (a) the *ortho*-atoms H(2) and H(6), where $\omega \neq |90|°$, (b) $M{-}P{-}C_i{-}C_o$ ($-\omega$) and (c) the apices associated with rings **A** and **B** which, for example flank the ligand L^1

the achiral complex-bound state, using molecular modelling techniques.

The potential energy surface of **1** is complicated, and in section A, we have sought primarily to characterise the inter ring–ring interactions which accompany a correlated arrangement. We demonstrate that the lowest energy conformation of **1** lies in a broad potential energy well, and an equally broad range of energetically acceptable phenyl ring orientations are accessible *via* independent P–C bond rotations. In sections B and C, we consider the effect upon the correlated conformations of **1** when coordinated to tetrahedral and trigonal-bipyramidal achiral metal centres, respectively. Using representative structures, we establish that the calculated minimum energy conformations (which compare well with the crystal) lie in broad potential energy wells, and in a manner reminiscent of the free ligand, a *range* of energetically tolerable phenyl ring orientations may also be adopted (*via* P–C bond rotation). Importantly, we show that the *apices* of the phenyl rings minimise inter ring–ligand interactions by adopting a staggered arrangement with respect to the ligands upon the metal. We then demonstrate that the minimum energy conformations adopted by the representative structures reflect an equilibrium between both inter ring–ligand and inter ring–ring interactions. We finally conclude that the equilibrium of intermolecular repulsive interactions is reflected in certain experimentally determined dihedral angles associated with the M–P bond.

Definitions

In order to study those steric factors which govern the conformations of triphenylphosphine in the free and metal-complex bound forms, it is necessary to define in an unambiguous fashion those geometric parameters which describe the orientation of the phenyl rings, both with respect to each other, and to those ligands attached to a metal centre. Figs. 2 and 3 define parameters which shall be referred to throughout these studies. It is convenient to describe the orientation of the phenyl ring attached to the phosphorus atom in a triphenylphosphine ligand in terms of the torsion angle $M{-}P{-}C_i{-}C_o$ [hereon referred to as ω, Fig. 2(a)]. When $\omega = 0°$, the bonds M–P and $C{-}H_o$ occupy the same plane, where H(2) is defined as being proximal, and H(6) distal to those ligands which are attached to the metal centre, M.

Fig. 2(b) depicts triphenylphosphine viewed along the axis defined by the P and *para*-carbon atom of a phenyl ring, the plane of which is oriented perpendicular to the reference plane. The correlated *clockwise* or *anti-clockwise* deviation of the torsion angle ω from 0° determines the helical chirality of the triphenylphosphine rotor. A negative value for ω corresponds to a *clockwise* torsion and therefore *clockwise* (*P*) helical chirality. A positive value for ω denotes an *anti-clockwise* torsion and an *anti-clockwise* (*M*) sense of helical chirality. In this preliminary study, we choose to limit our discussion to the conformations of triphenylphosphine coordinated to an achiral metal centre [*i.e.* $L^1 = L^2 = L^3$, Fig. 2(c)]. Consequently, we arbitrarily choose to consider the *clockwise* (*i.e.* $-\omega$) helical configuration of **1**. The arguments put forward here for the *clockwise* configuration at an achiral metal centre apply equally to the degenerate enantiomeric *anti-clockwise* case.

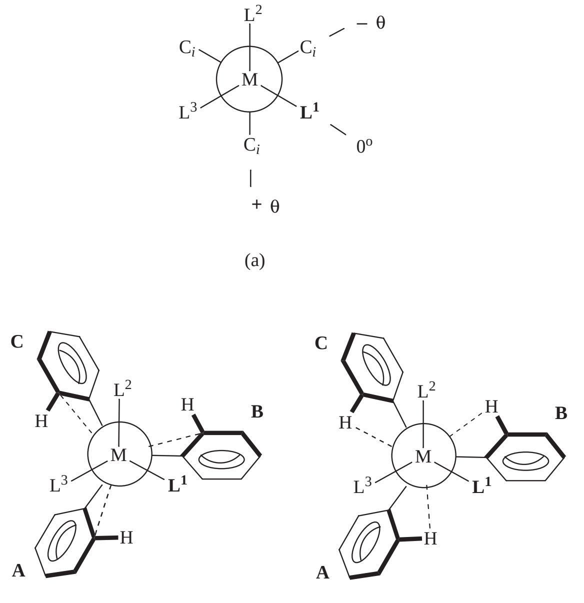

(a)

(b) (c)

Fig. 3 Newman projections along the M–P bond demonstrating the torsion angles (a) $L^1{-}M{-}P{-}C(1)_i$ (θ_{C_i}), (b) $L^1{-}M{-}P{-}C(2)_o$ (θ_{C_o}), and (c) $L^1{-}M{-}P{-}H(2)_o$ (θ_{H_o})

Fig. 2(c) depicts a triphenylphosphine ligand possessing *clockwise* ($-\omega$) helical chirality viewed along the axis defined by metal M (with associated ligands L^{1-3}) and phosphorus atoms. When $\omega \neq |90|°$, the *ortho*-hydrogen atom (and associated carbon atom) proximal to the metal centre M, constitute the *apex* of the phenyl blade. With respect to a given ligand, such as L^1, phenyl rings **A** and **B** present an apex. Indeed, each ligand L^{1-3} will be flanked by the apex of two adjacent phenyl rings. In order to monitor the displacement of the C_i, and C_o/H_o atoms (the latter of which constitute an apex) of ring **A** with respect to ligand L^1 for example, we have defined the torsion angles $L^1{-}M{-}P{-}C(1)$ (θ_{C_i}), $L^1{-}M{-}P{-}C(2)$ (θ_{C_o}) and $L^1{-}M{-}P{-}H(2)$ (θ_{H_o}) [Fig. 3(a)–(c), respectively].

A sawhorse projection of the perfectly staggered minimum energy conformation of 2,2,3,3-tetramethylbutane is shown in Fig. 4(a). The potential energy is clearly a function of the dihedral angle $H_3C{-}C{-}C{-}CH_3$; the barrier to rotation being occasioned by the fact that eclipsing methyl groups incur the maximum steric compression. A given CH_3 group upon C(2) for example, will prefer to be oriented [*via* C(2)–C(3) bond rotation] proximal to the point of minimum vicinal steric compression bisecting two geminal CH_3 groups upon C(3). Indeed, a continuum of minimum steric compression delimited by the C(2)–C(3) bond axis exists at all points within the plane bisecting all geminal CH_3 groups [Fig. 4(a)]. We have termed a plane incorporating all points of minimum steric compression the *plane of nadir energy*. Thus, the minimum energy conformation of 2,2,3,3-tetramethylbutane is consistent with all six CH_3 groups being oriented proximal to a plane of nadir energy. This is a trivial definition in the case of 2,2,3,3-tetramethylbutane, as the distance between the vicinal CH_3 groups is essentially fixed. It is conventional therefore to describe the minimum vicinal steric compression between the spherically symmetric CH_3 groups in terms of points in space.

Fig. 4(b) shows the three planes of nadir energy described by adjacent ligands L, coordinated to a tetrahedral or trigonal-

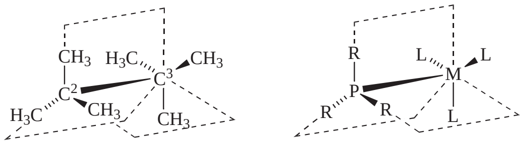

(a) (b)

Fig. 4 The planes of nadir energy described by (a) the CH_3 groups upon C(3) within 2,2,3,3-tetramethylbutane, and (b) the ligands L, upon an achiral metal centre, M

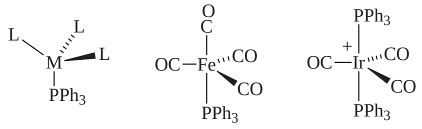

7 8

	M	L
2	Al	CH_3
3	Mn	NO
4/5/6	Ni^-	Cl/Br/I

Fig. 5 The achiral complexes **2**–**8**

bipyramidal achiral metal centre. In the case of $R = CH_3$ [*i.e.* $P(CH_3)_3$], the spherically symmetric CH_3 groups will prefer to be oriented (*via* P–M bond rotation) proximal to a plane of nadir energy, thereby staggering the P–C and M–L bonds. Again, this constitutes a trivial application of the definition. However, in the case of R = Ph (*i.e.* PPh_3), the atoms associated with a ring apex will prefer to be orientated proximal to the planes of nadir energy; the ring apices and not the P–C bonds will be staggered with respect to the M–L bonds. As the torsion angle ω varies, the position of the atoms associated with a ring apex will move with respect to the plane of nadir energy. Therefore, in the context of this study, discussions related to the steric compression imposed by two flanking ligands upon a phenyl ring apex are more appropriately described within planes.

Several criteria have guided our choice of metal complex for this particular study. In the first instance, we have chosen to examine the conformational preferences of the triphenylphosphine ligand coordinated to a metal centre possessing C_3 symmetry. Consequently, we are restricted in our analyses to complexes of tetrahedral or trigonal-bipyramidal geometry. For simplicity, we have considered complexes in which the ligands (other than triphenylphosphine) possess the highest symmetry possible. Our choice of complexes **2**–**8** (Fig. 5) allows us to examine how variations in both the complex geometry, and the nature of the ligand influence the conformational preferences of **1**. Our choice of **8** allows us to extend[1] this study at a later date to encompass prochiral metal complexes.

Results and discussion

A Triphenylphosphine

Before analysing the conformations of **1** when coordinated to a metal centre, it is instructive to consider the case of triphenylphosphine alone. In doing so, the manner in which the phenyl rings interact with each other can be considered[4] before introducing the additional non-bonded interactions derived from the ligands associated with a metal centre. The X-ray crystal structure of **1** (Fig. 1) has been reported previously,[11a–d] and values of $\omega_{A\text{–}C}$ are presented in Table 1.

Table 1 Crystallographically derived data for **1**–**8**

Structure (refcode)	ω/° A	B	C	$+\theta$(cryst.)[a]/° C_i	C_o	H_o
1 (PTRPHE)[11a]	−56	−29	−24			
1 (PTRPHE01-03)[11b–d]	−56	−27	−25			
2 (KIFSOH)[11e]	−39	−39	−38	80	64	53
3 (PNOMNA)[11f]	−44	−48	−47	115	95	81
4 (DAJCIA)[11g]	−54	−39	−27	64	47	34
5 (ASBRNI)[11h]	−35	−26	−34	72	59	49
6 (PASPNI)[11i]	−53	−35	−51	77	59	44
7 (PPTCFE)[11j]	−47	−44	−41	84	66	54
8 (KISGEY)[11k]	−53	−39	−37	78	60	48
	−46	−42	−49			

All values of $\omega_{A\text{–}C}$ have been normalised to the clockwise rotor sense. In defining $\omega = \sigma_{nb}\text{–P–}C_i\text{–}C_o$ in **1**, σ_{nb} has been designated as the vector perpendicular to the reference plane and incident upon the P atom. [a] Except for **2**, average value cited.

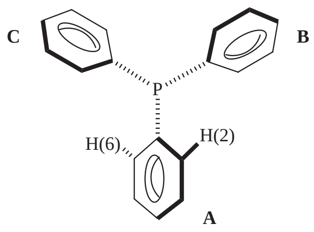

Fig. 6 The *ortho*-hydrogen atoms H(2) and H(6) viewed along the σ_{nb}–P axis

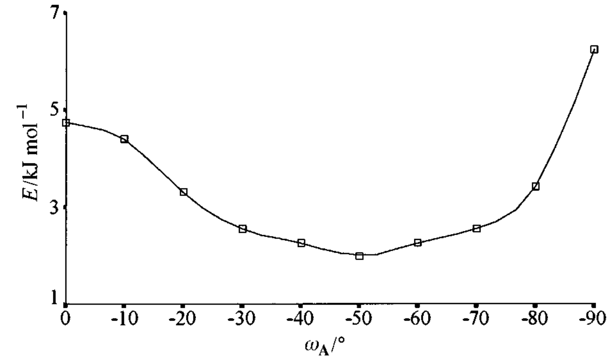

Fig. 7 The conformational energy of **1**

Molecular modelling studies using the Chem-X package, employing van der Waals interaction energy calculations, have been used to investigate the thermodynamically preferred conformations of **1**. The crystallographically derived coordinates of **1**[11d] provided the starting point for our studies. The structure was modified by setting ω of rings **A**–**C** (Fig. 6) = 0° thereby affording a C_{3v} symmetrical starting point. The torsion angle ω_A was driven through the range $0 \rightarrow -90°$ in 10° increments. Analysis outside this range corresponds to an inversion of the rotor-sense and is therefore irrelevant as energetically degenerate conformations are produced.[2] At each increment, the van der Waals interaction energy of the structure was allowed to minimise by independent rotation about the P–C_i bonds associated with rings **B** and **C** until the default energy convergence criteria were achieved. The calculated change in energy associated with driving ω_A ($0 \rightarrow -90°$) is presented in Fig. 7. The variation of $\omega_{B/C}$ associated with driving ω_A through this range is also presented in Fig. 8.

The calculated energy profile presented in Fig. 7 is in good qualitative agreement with previous studies using semi-empirical methods,[2,11d] which conclude that the barrier to P–C bond rotation is low. A broad energy minimum was identified for **1**, corresponding to $\omega_A = -40 \rightarrow -60°$ and centred upon $\omega_A = ca.\ -50°$. Energy maxima were identified at $\omega_A = 0$ and $-90°$. As ω_A is driven through $0 \rightarrow -40°$, the corresponding torsion angles for rings **B** and **C** (ω_B and ω_C) converge to approximately −50° (Fig. 8). Thereafter, the values of ω_B and ω_C remain relatively unperturbed as ω_A is driven through *ca.* $-40 \rightarrow -60°$. The calculations suggest therefore that the optimum value of $\omega_{A\text{–}C}$ is approximately −50°, thereby affording an overall C_3 symmetry for the structure. Furthermore, the broad ($\omega_A = ca.\ -40 \rightarrow -60°$) and shallow energy minimum associated with driving the P–C bond of ring **A**, in concert with the

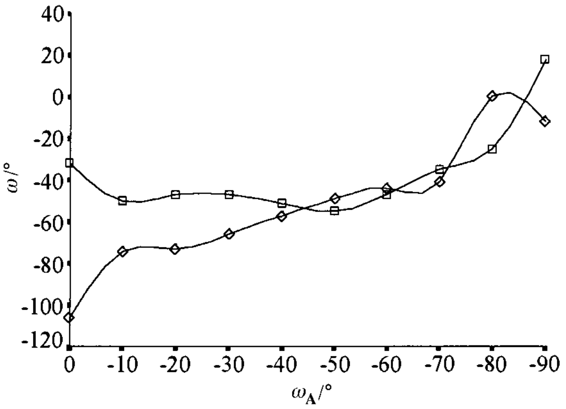

Fig. 8 The variation of ω_B (□) and ω_C (◇) with ω_A in **1**

absence of a notable perturbation of the torsion angles $\omega_{B/C}$ in the same range, suggests that a degree of mutually independent rotation about all three P–C bonds of **1** is energetically tolerable.

As ω_A is driven through $0 \rightarrow -35°$ and $-70 \rightarrow -90°$, ω_B and ω_C deviate markedly from their optimum value (Fig. 8). In order to appreciate the intramolecular interactions attending these energy maxima, a brief analysis of the manner in which the *ortho*-hydrogen atoms of ring **A** impinge upon the adjacent phenyl rings **B** and **C** is warranted. As expected, the tetrahedral geometry about the P atom of **1** (σ_{nb}–P–C = 115.5°) enforces intramolecular distances of the type ring **A** H(6)···ring **C** < ring **A** H(2)···ring **B** as ω_A is driven $0 \rightarrow$ *ca.* $-85°$. Therefore, it can be anticipated that in this range the steric requirements of atoms of type H(6) will be more demanding than those of type H(2). As ω_A is driven through $0 \rightarrow -10°$, the degree to which H(6) of ring **A** may impinge upon ring **C** is minimal. Consequently, ring **C** may relax into an approximately perpendicular orientation with respect to ring **A** (Fig. 8). In doing so, H(6) of ring **C** impinges markedly upon ring **B**. In order to relieve this sterically demanding interaction, ring **B** is forced to adopt an almost perpendicular orientation with respect to ring **C**. It is the relief of the intramolecular steric compression imposed upon ring **B** by ring **C** as ω_A is driven, which facilitates the observed energy minimum.

The calculated lowest energy conformation of **1** (ω_{A-C} = *ca.* $-50°$) is such that the P–C bond of each phenyl ring lies in the plane of the impinging phenyl ring [Fig. 9(a)]. The dominant interaction occurs between the atoms H(6) and C(1) of adjacent phenyl rings. Rotation about a single P–C bond invokes additional steric compression between the H(6) and C(2) atoms of adjacent rings; however as can be seen from Fig. 8, small deviations from the equilibrium structure may be easily accommodated. The intramolecular energy of the system rises to a maximum as ω_A is driven through *ca.* $-70 \rightarrow -90°$ (Fig. 7). It is within this range that the distance between both H_o atoms of ring **A** and the C(1) atoms of the adjacent rings **B** and **C** approach a minimum. Consequently, rings **B** and **C** are forced into essentially vertical orientations (Fig. 8) in order to accommodate the intramolecular infringement. As $\omega_A \rightarrow -90°$, $|\omega_{B/C}| \rightarrow 0°$ and an energy maximum accompanies what amounts to the two-ring flip stereoisomerisation process.[4]

In conclusion, for **1** in the free state, calculations suggest that the optimum value of ω which obviates energetically demanding intramolecular interactions is *ca.* $-50 \pm 10°$. It is clear that the intramolecular interaction which governs conformational stability is associated with an *ortho*-atom of type H(6) and an *ipso*-carbon atom of a neighbouring phenyl ring. The crystallographically derived values of ω_{A-C} are summarised in Table 1. The value of ω_A adopted in the crystal ($\omega_A = -56°$) correlates reasonably well with the calculation. However, the crystallographically derived values for rings **B** and **C** ($\omega_{B/C} = -27/-25°$) are at variance with the calculated energy minimum, suggesting that these two rings are perturbed in the crystal. This perturbation places the H(6) atoms of rings **B** and **C** closer together, thereby invoking a steric penalty otherwise absent in the calculated minimum energy structure. Full minimisation of **1** corroborates our assertion that the global minimum corresponds to the C_3 symmetric structure whereby ω_{A-C} = *ca.* $-50°$.‡ We and others[2,11d] have noted the disparity between the calculation and the crystal.§ Calculations[12] and gas phase basicity measurements[13] of arylphosphines and their nitrogen analogues suggest that the rehybridisation of phosphorus *via* the dispersion of σ_{nb} electron density, although attendant,[14] is less marked than for nitrogen. Solid state ^{31}P NMR analysis of **1** suggests a large amplitude of motion about the P–C bonds.[15] This observation is wholly consistent with our calculations which suggest that the energy barriers to P–C bond rotation are low. Therefore, as a stereoelectronic effect for ring **A** is expected to be weak, the observed distortion of molecular symmetry in the crystal is consistent with packing effects.[7a,11a,d]

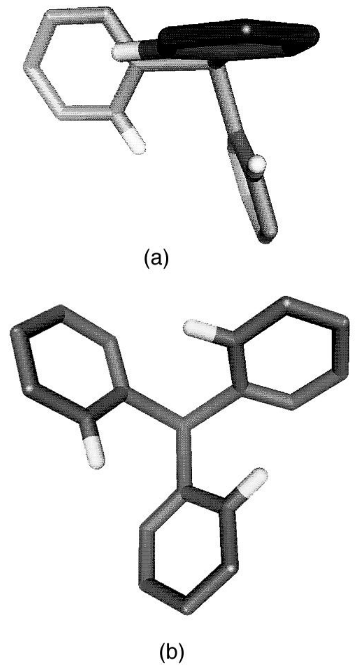

(a)

(b)

Fig. 9 The calculated lowest energy conformation of **1** as viewed along (a) the C–P bond axis of one phenyl ring and (b) the P–σ_{nb} axis. Atoms of type H(6) alone are displayed.

B Triphenylphosphine coordinated to a tetrahedral metal centre

For the case of triphenylphosphine coordinated to a tetrahedral metal centre, we consider complex **2** as a representative example. In a manner similar to that described earlier, the crystallographically derived coordinates of **2**[11e] provided the starting point for our calculations. The structure was modified by firstly setting the torsion angles $\omega_{A-C} = 0°$ and $\theta_{C_i} = 180°$. The torsion angle ω_A was driven through the range $0 \rightarrow -90°$ in 10° increments, and the torsion angles $\omega_{B/C}$ were also driven

---

‡ Consistent with the observation that the equilibrium structure of an isolated $OPPh_3$ fragment is also close to a symmetric propeller shape (E. Bye, W. B. Schweizer and J. D. Dunitz, *J. Am. Chem. Soc.*, 1982, **104**, 5393).

§ The values of ω_{A-C} for $OPPh_3$ in the crystal are very similar to those observed for **1** (C. P. Brock, W. B. Schweizer and J. D. Dunitz, *J. Am. Chem. Soc.*, 1985, **107**, 6964). Here, a stereoelectronic argument has been invoked in order to rationalise the apparent 'flattening' ($\omega_A = -60°$) of one ring with respect to the reference plane. Interestingly, this 'flattened' ring possesses a significant librational amplitude in the crystal (J. D. Dunitz, E. F. Maverick and K. N. Trueblood, *Angew. Chem., Int. Ed. Engl.*, 1988, **27**, 880), suggesting that long-range packing forces are being opposed by a weak stereoelectronic preference of one phenyl ring to be oriented perpendicular to the P–O bond.

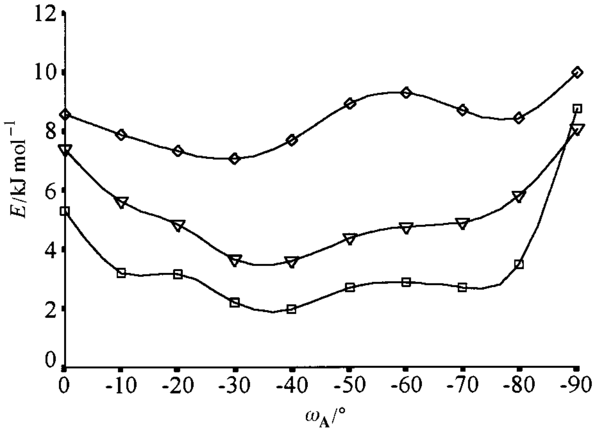

Fig. 10 The calculated conformational energy of complexes **2** (▽), **7** (□) and **8** (◇). A comparison between the relative energies of **2**, **7** and **8** is not implied.

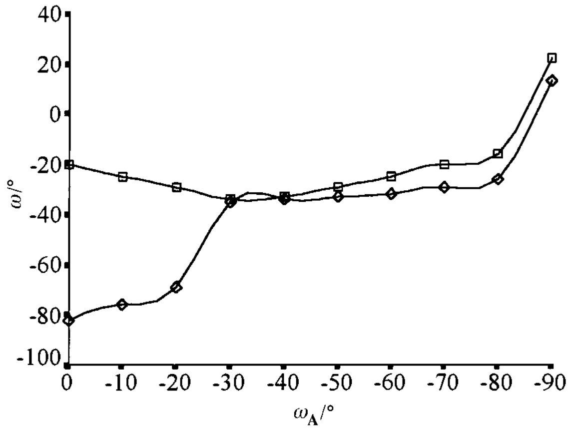

Fig. 11 The variation of ω_B (◇) and ω_C (□) with ω_A in **2**

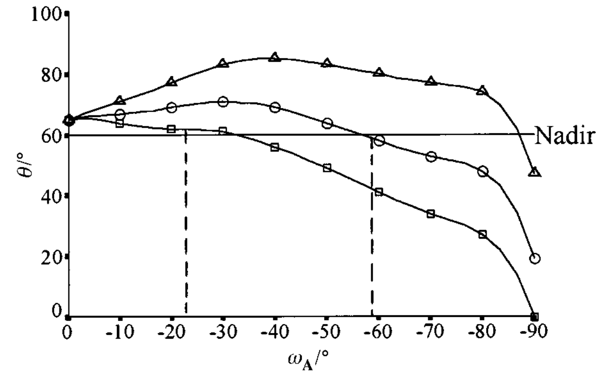

Fig. 12 The variation of θ_{C_i} (△), θ_{C_o} (○) and θ_{H_o} (□) with ω_A in **2**

(0→−90°, 4° increments) with concomitant minimisation of all rotatable bonds until the default energy convergence criteria were achieved. The calculated change in intramolecular energy associated with driving the torsion angle ω_A through the range 0→−90° is presented in Fig. 10. The variation of ω_B and ω_C arising as ω_A is driven through the same range is presented in Fig. 11.

One broad energy minimum was found to be centred upon $\omega_A = $ *ca.* −37°, which is in accord with the crystal (Table 1). It would appear that coordination of **1** to a tetrahedral metal centre possessing sterically demanding ligands will decrease the average value of ω from *ca.* −50 ± 10° (Fig. 7) to *ca.* −40 ± 10° (Figs. 10 and 11). In this case, it is clear that ligands L^{1-3} impose a restriction upon P–C bond rotation which is otherwise absent in the free ligand. In contrast, the crystallographically observed values of ω_{A-C} in the tetrahedral complex $[Mn(PPh_3)(NO)_3]$ **3** (Table 1) are comparable to those of the free ligand **1**. This is consistent with the NO ligand being less sterically demanding than the CH_3 ligand, and therefore presenting less of an impediment to P–C bond rotation. Returning once again to **2**, Fig. 11 demonstrates that in the range $\omega_A = $ *ca.* −30→−50°, the torsion angles ω_B and ω_C are essentially unperturbed from $\omega = $ *ca.* −30°. This suggests that the relative orientations of rings **B** and **C** are effectively isolated from and independent of ring **A** within this range. This is in marked contrast to the free ligand **1** (Fig. 8). In the same range, ring **C** is allowed to relax markedly ($\omega_C > -60°$) in the absence of steric compression from ring **A**.

In the case of **2**–**8**, where L^{1-3} are identical, the volume of space between two adjacent ligands will be symmetrical about the plane which bisects them. Furthermore, an atom or group of atoms which impinges upon the volume of space flanked by two ligands will prefer to be oriented proximal to the plane of minimal steric compression, *i.e.* the plane of nadir energy. Therefore, the plane of nadir energy for complexes **2**–**8** will be coincident upon $|\theta| = 60°$. It is important to note that the steric influence of two adjacent ligands about the plane of nadir energy will depend upon: (i) the nature (size) of the ligands, (ii) the geometry about the metal, and (iii) the P–M bond length, and is expected to diminish along the M–P bond axis. Fig. 12 describes the calculated effect upon the torsion angles $\theta_{C_i/C_o/H_o}$ associated with ring **A** as ω_A is driven (0→−90°). The magnitudes of the torsion angles $\theta_{C_i/C_o/H_o}$ derived from the crystal are in good agreement with the calculation.

The orientation adopted by the phenyl rings of the triphenylphosphine ligand in **2** will be governed by the ability of the impinging atoms associated with the apex of phenyl ring **A** (for example) to be placed proximal to the plane of nadir energy which bisects ligands L^1 and L^3. This may be achieved *via* P–C and M–P bond rotations. For a given value of ω_A which ensures that the impinging atom associated with a phenyl ring apex is of the type H(2) alone, one can expect H(2) to be oriented (*via* M–P bond rotation) proximal to the plane of nadir energy. Thus, if one considers the apex of ring **A** relative to the ligand L^1, one would expect $\theta_{H_o} = +60°$ and $\theta_{C_o/C_i} > +60°$. This is indeed found to be the case for values of $\omega_A = -20 \rightarrow -30°$ (Fig. 12). Furthermore, it can be seen that $\theta_{C_i} > +60°$ reflects rotation about the M–P bond in response to the steric compression imposed by adjacent ligands upon the apex of ring **A**. As ω_A is driven −30→−50° (Fig. 10), the total van der Waals energy of the system approaches a minimum. Both of the atoms associated with the C(2)–H(2) bond now constitute the interacting apex of the phenyl ring. Consequently, both atoms attempt to lie proximal to the plane of nadir energy, resulting in $\theta_{H_o} < +60° < \theta_{C_o}$. In brief, the lowest energy conformation of **2** is consistent with the apices [*i.e.* C(2)–H(2)] of all three phenyl rings lying proximal to the plane of nadir energy. The range of ω delimited by the intersection of the plane of nadir energy ($\theta = +60°$) and the curves associated with θ_{C_o/H_o} (*i.e.* vertical dashed lines, −20→−60°, Fig. 12) is significant. This range corresponds to the energetically accessible (Fig. 10) orientations available to the phenyl rings of the PPh_3 fragment in **2**.

As discussed previously, θ_{C_i} must increase (*via* M–P bond rotation) within the range $\omega_A = 0 \rightarrow -40°$ in order to orient the atoms associated with the ring apex proximal to the plane of nadir energy. Thus, an increase in θ_{C_i} accompanies the minimisation of inter ring–ligand interactions. For $\omega_A > -40°$, the diminished steric influence of the adjacent ligands upon the ring apex is reflected in a decrease in the magnitude of θ_{C_i}. However, as the inter **A** ring–ligand interactions diminish, sterically demanding inter ring–ring interactions give rise to an increase in the total energy of the complex. Therefore, θ_{C_i}(max.) correlates with the optimum value of ω which minimises *both*

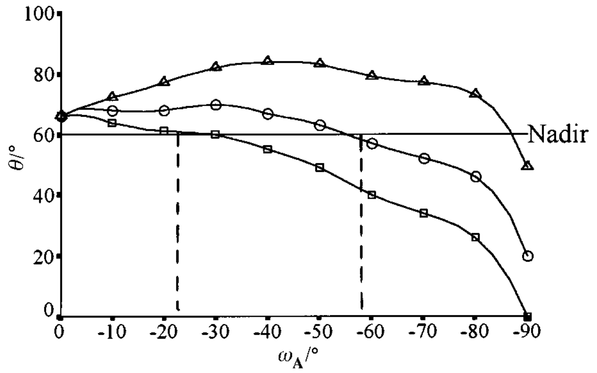

Fig. 13 The variation of θ_{C_i} (△), θ_{C_o} (○) and θ_{H_o} (□) with ω_A in **7**

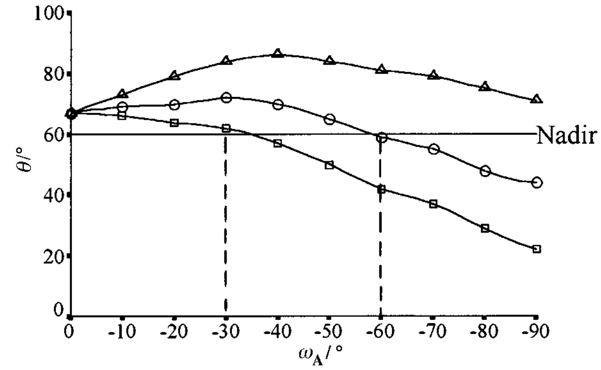

Fig. 14 The variation of θ_{C_i} (△), θ_{C_o} (○) and θ_{H_o} (□) with ω_A in **8**

inter ring–ring and inter ring–ligand interactions. In the calculation θ_{C_i} achieves a maximum value of +84° at $\omega_A = -40°$. Allowing for the small discrepancies between the perfectly symmetrical structure used for our calculations and the crystal structure, θ_{C_i}(max.) = θ_{C_i}(cryst.) (Table 1). Therefore, θ_{C_i}(cryst.) serves as an experimental indicator of the minimisation of inter ring–ring/ring–ligand repulsive interactions.

As previously indicated, the NO ligands in **3** exert relatively little steric influence upon the plane of nadir energy. This is evident not only from $\omega_{A\text{-}C}$ (Table 1), but more notably from θ_{C_i}(cryst.). The P–C and Mn–NO bonds are allowed to adopt an essentially eclipsed arrangement in the absence of any steric compulsion to orient a ring apex proximal to the nadir plane. As expected, an increase in the steric compression about the plane of nadir energy in a series such as $[Ni(PPh_3)_2(Cl)_3]^-$ **4**→$[Ni(PPh_3)_2(Br)_3]^-$ **5**→$[Ni(PPh_3)_2(I)_3]^-$ **6** is reflected in a concomitant increase in θ_{C_i}(cryst.) (64→77°, Table 1). Clearly, as the steric pressure about the plane of nadir energy increases, so a greater degree of M–P bond rotation is required in order to accommodate all of the atoms of the ring apex. For example, in the case of **4**, the Cl ligands exert little compulsion upon the triphenylphosphine ligand to orient the atoms associated with the ring apexes proximal to the plane of nadir energy. This is not the case for **5**→**6**, where the largest atom of the apex (C_o) is compelled to lie within the plane of nadir energy defined by the sterically demanding Br and I ligands.

C Triphenylphosphine coordinated to a trigonal-bipyramidal metal centre

For the case of triphenylphosphine coordinated to a trigonal-bipyramidal metal centre, we consider complex **7** as a representative example. In a similar manner to that described for complex **2**, the crystallographically derived coordinates of **7**[11j] provided the starting point for our calculations. The calculated change in intramolecular energy associated with driving the torsion angle ω_A through the range 0→−90° has been superimposed upon Fig. 10. A comparison between the relative energies of **2** and **7** is not implied. One broad energy minimum was identified which is in good agreement with the crystal (Table 1). The plot of ω_A *versus* $\omega_{B/C}$ for **7** is essentially superimposable upon that for complex **2** in Fig. 11. The torsion angles $\theta_{C_i/C_o/H_o}$ of **7** were calculated (Fig. 13) and were also found to be superimposable upon those presented for **2** (Fig. 12). This implies that the steric compression about the plane of nadir energy in **2** is comparable to that of **7**. A similarity is to be expected when one considers that the steric compression imposed by both a shorter P–M bond length and a trigonal-bipyramidal geometry in **7** will be off-set by a decrease in the van der Waals radii of the ligand (CH_3→CO). As noted for complex **2**, θ_{C_i}(max.) corresponds to the optimum value of ω_A in the crystal which minimises the magnitude of the ring–ring and ring–ligand interactions. Again, it should be emphasised that the range of ω delimited by the intersection of the plane of nadir energy ($\theta = +60°$) and the curves associated with θ_{C_o/H_o} (*i.e.* vertical dashed lines, Fig. 13) correspond to the energetically accessible orientations (Fig. 10) available to the phenyl rings of the PPh_3 ligand in **7**.

Changing the nature of the metal centre in **7** (Fe) to **8** (Ir) has the effect of increasing the M–P (Δ = +0.12 Å) and M–CO (Δ = +0.11 Å) bond lengths, respectively. Therefore, we investigated whether the relief of intramolecular non-bonded interactions in complex **8** would be manifested in the calculation. In a similar manner to that described for complex **2**, the crystallographically derived coordinates of **8**[11k] provided the starting point for our calculations. For simplicity, calculations were performed upon one triphenylphosphine ligand alone; the other being replaced with a CO ligand. The calculated change in intramolecular energy associated with driving the torsion angle ω_A of **8** through the range 0→−90° has been superimposed upon Fig. 10. Again, a comparison between the relative energies of **2**, **7** and **8** is not implied. A very broad energy minimum was found to be centred upon ω_A = *ca.* −30°. With the exception of the sharp deviation of $\omega_{B/C}$ at $\omega_A = -90°$, the plot of ω_A *versus* $\omega_{B/C}$ for **8** is superimposable upon that of complex **2** (Fig. 11). This is presumably a manifestation of the decreased steric impediment to phenyl ring relaxation in complex **8** relative to complexes **2** and **7**.

Fig. 14 describes the effect upon the values of θ as ω_A is driven (0→−90°) in **8**. The magnitude of the torsion angles $\theta_{C_i/C_o/H_o}$ derived from the crystal are in good agreement with the calculation. The sharp deviation observed at $\omega_A = -80°$ for complexes **2** and **7** (Figs. 12 and 13, respectively) is not observed for **8**. Furthermore, the range of values of ω_A delimited by the intersection of the plane of nadir energy ($\theta = +60°$) and the curves θ_{C_o/H_o} (*i.e.* vertical dashed lines, ω_A = *ca.* −30→−60°, Fig. 14) is less for **8** than **7**. The latter observation in particular is indicative of the diminished steric influence of the ligands in **8** upon the nadir plane. Furthermore, it is apparent from θ_{C_i}(cryst.) (Table 1) that a smaller degree of M–P bond rotation is required to orient the largest atom of the apex proximal to the plane of nadir energy.

In conclusion, the conformations adopted by **2**, **7** and **8** in the crystal are consistent with the calculated minimum energy structures generated using van der Waals energy calculations. It is reasonable to assume therefore, that the dominant influences upon the conformations adopted by **1** in such complexes are non-bonded repulsive interactions. The minimum energy conformations adopted by complex-bound **1** represent a balance between two steric influences. Firstly, the phenyl rings within a correlated arrangement will attempt to minimise the inter ring–ring interactions *via* P–C bond rotations. Secondly, inter ring–ligand interactions are minimised *via* the orientation of a ring apex proximal to the plane of nadir energy. These orientations can be achieved *via* a relatively wide range of values of ω (P–C bond rotation), but a much smaller range of values of θ_{C_i} (M–P bond rotation). It has been established that both calculated [θ_{C_i}(max.)] and experimental [θ_{C_i}(cryst.)] parameters are in accord with the equilibrium established between both inter ring–ring and inter ring–ligand repulsive interactions. An extension of this methodology to the analysis of prochiral and stereogenic octahedral metal complexes will follow in due course.[1]

Experimental

Data retrieval

Crystal structures containing appropriate molecular fragments were located within the Cambridge Structural Database (CSD) using the QUEST program.[16] Data for these molecular structures were retrieved from the April 1997 release of the CSD in which the master data file contained 167 797 entries.

Molecular modelling calculations

All molecular modelling calculations were conducted using the Chem-X package (January 1997) supported on the Windows 95 platform using a Pentium personal computer. The van der Waals energy (E_{vdW}) calculation within Chem-X is a subset of the full molecular mechanics calculation which assumes that all bond lengths and angles are fixed and idealised and that the energy depends only upon the non-bonded (including 1,4) interactions. For all calculations, idealised structures have been used, with average bond lengths and angles being derived from the appropriate crystallographic data. Phenyl rings were treated as rigid bodies of $D_{6\mathrm{h}}$ symmetry. The van der Waals energy (E_{vdW}) considers contributions from the torsion (V_{tor}), electrostatic (V_{el}) and non-bonded (V_{nb}) terms [as defined in eqn. (1)],

$$E_{\mathrm{vdW}} = V_{\mathrm{tor}} + V_{\mathrm{el}} + V_{\mathrm{nb}} \qquad (1)$$

but without the range of functional forms and parameters available in the full molecular mechanics calculation. Consequently, the calculations described herein can only be viewed as qualitative in nature.

Generic barrier constants were employed in the basic form of the torsion term (V_{tor}). The electrostatic contribution (V_{el}) is computed as a monopole–monopole interaction using Coulomb's law. The van der Waals interaction potential (V_{nb}) within the software package is that of Del Re *et al.*,[17] and takes the form given in eqn. (2).

$$V_{\mathrm{nb}} = [A \exp(-Br)]r^{-D} - Cr^{-6} \qquad (2)$$

In all calculations, steric contributions to V_{nb} from the metal atom were not included because of the lack of adequate parameterisation. However, steric contributions from the metal centre upon the conformations of the triphenylphosphine ligand are considered to be negligible. The van der Waals energy was minimised for all conformations by independent rotations about all other single bonds (except those to CO ligands and hydrogen atoms) within the molecule.

Acknowledgements

We thank Professor S. Ramdas (Imperial College) for helpful suggestions in the preparation of this manuscript.

References

1 Part 2. Triphenylphosphine coordinated to achiral, prochiral and stereogenic octahedral metal centres, J. F. Costello and S. G. Davies, in preparation.
2 C. P. Brock and J. A. Ibers, *Acta Crystallogr., Sect. B*, 1973, **29**, 2426.
3 R. S. Cahn, C. Ingold and V. Prelog, *Angew. Chem., Int. Ed. Engl.*, 1966, **5**, 385.
4 K. Mislow, *Acc. Chem. Res.*, 1976, **9**, 26; M. R. Kates, J. D. Andose, P. F. Finocchiaro, D. Gust and K. Mislow, *J. Am. Chem. Soc.*, 1975, **97**, 1772; D. Gust and K. Mislow, *J. Am. Chem. Soc.*, 1973, **95**, 1535; E. E. Willie, D. S. Stephenson, P. Capriel and G. Binsch, *J. Am. Chem. Soc.*, 1982, **104**, 405.
5 J. M. Brown and K. Mertis, *J. Organomet. Chem.*, 1973, **47**, 5; G. Hunter, T. J. R. Weakley and W. Weissensteiner, *J. Chem. Soc., Dalton Trans.*, 1987, 1545; J. A. Chedek, G. Hunter, R. L. Mackay, P. Kremminger, K. Schlogel and W. Weissensteiner, *J. Chem. Soc., Dalton Trans.*, 1990, 2001; A. Bayler, G. A. Bowmaker and H. Schmidbaur, *Inorg. Chem.*, 1996, **35**, 5959.
6 A. G. Orpen, *Chem. Soc. Rev.*, 1993, **22**, 191; S. E. Garner and A. G. Orpen, *J. Chem. Soc., Dalton Trans.*, 1993, 533.
7 (*a*) H. Brunner, B. Hammer, C. Kruger, K. Angermund and I. Bernal, *Organometallics*, 1985, **4**, 1063; (*b*) for a similar analysis of aminophosphines, see H. Brunner, H. Weber, I. Bernal and G. M. Reisner, *Organometallics*, 1984, **3**, 163.
8 J. Polowin, S. C. Mackie and M. C. Baird, *Organometallics*, 1992, **11**, 3724.
9 H. Brunner, R. Oeschey and B. Nuber, *Angew. Chem., Int. Ed. Engl.*, 1994, **33**, 866.
10 S. G. Davies, A. E. Derome and J. P. McNally, *J. Am. Chem. Soc.*, 1991, **113**, 2854, and references cited therein. See also, S. C. Case-Green, J. F. Costello, S. G. Davies, N. Heaton, C. J. R. Hedgecock, V. M. Humphreys, M. R. Metzler and J. C. Prime, *J. Chem. Soc., Perkin Trans. 1*, 1994, 933; S. J. Cook, J. F. Costello, S. G. Davies and H. T. Kruk, *J. Chem. Soc., Perkin Trans. 1*, 1994, 2369; J. F. Costello, S. G. Davies, R. M. Highcock, M. E. C. Polywka, M. W. Poulter, T. Richardson and G. G. Roberts, *J. Chem. Soc., Dalton Trans.*, 1997, 105.
11 (*a*) J. J. Daly, *J. Chem. Soc.*, 1964, 3799; (*b*) B. J. Dunne and A. G. Orpen, *Acta Crystallogr., Sect. C*, 1991, **47**, 345; (*c*) A. N. Chekhlov, *Kristallografiya*, 1993, **38**, 79; (*d*) J. Bruckmann, C. Kruger and F. Lutz, *Z. Naturforsch., Teil B*, 1995, **50**, 351; (*e*) D. A. Wierda and A. R. Barron, *Polyhedron*, 1989, **8**, 831; (*f*) R. D. Wilson and R. Bau, *J. Organomet. Chem.*, 1980, **191**, 123; (*g*) M. Brenndorfer, H. A. Brune, T. Debaerdemaeker and R. Hemmer, *Z. Naturforsch., Teil B*, 1985, **40**, 357; (*h*) L. R. Hanton and P. R. Raithby, *Acta Crystallogr., Sect. B*, 1980, **36**, 2417; (*i*) R. P. Taylor, D. H. Templeton and W. DeW. Horrocks, Jr., *Inorg. Chem.*, 1968, **7**, 2629; (*j*) P. E. Riley and R. E. Davis, *Inorg. Chem.*, 1980, **19**, 159; (*k*) S. L. Randall, J. S. Thompson, L. A. Buttrey, J. W. Ziller, M. R. Churchill and J. D. Atwood, *Organometallics*, 1991, **10**, 683.
12 S. Ikuta, P. Kebarle, G. M. Bancroft, T. Chan and R. J. Puddephatt, *J. Am. Chem. Soc.*, 1982, **104**, 5899; D. G. Gilheany, *Chem. Rev.*, 1994, **94**, 1339.
13 S. Ikuta and P. Kebarle, *Can. J. Chem.*, 1983, **61**, 97.
14 T. Schaefer, R. Sebastian and F. E. Hruska, *Can. J. Chem.*, 1993, **71**, 639.
15 G. H. Penner and R. E. Wasylishen, *Can. J. Chem.*, 1989, **67**, 1909.
16 F. H. Allen and O. Kennard, *Chemical Design Automation News*, 1993, **8**, 31.
17 G. Del Re, E. Gavuzzo, E. Giglio, F. Lelj, F. Mazza and V. Zappia, *Acta Crystallogr., Sect. B*, 1977, **33**, 3289.

Paper 7/08014J
Received 6*th November* 1997
Accepted 15*th April* 1998